

Dimensionality and confinement effects in δ -doped Pd(Fe) layers

This article has been downloaded from IOPscience. Please scroll down to see the full text article.

2010 J. Phys.: Condens. Matter 22 236004

(<http://iopscience.iop.org/0953-8984/22/23/236004>)

View [the table of contents for this issue](#), or go to the [journal homepage](#) for more

Download details:

IP Address: 129.252.86.83

The article was downloaded on 30/05/2010 at 08:52

Please note that [terms and conditions apply](#).

Dimensionality and confinement effects in δ -doped Pd(Fe) layers

Evangelos Th Papaioannou, Vassilios Kapaklis, Andrea Taroni, Moreno Marcellini and Björgvin Hjörvarsson

Department of Physics and Astronomy, Materials Physics Division, Uppsala University, Box 516, 751 20 Uppsala, Sweden

Received 9 November 2009, in final form 31 March 2010

Published 26 May 2010

Online at stacks.iop.org/JPhysCM/22/236004

Abstract

We address the dimensionality aspects of the magnetic ordering in δ -doped Pd(Fe) structures. The key property we investigate, via magneto-optic Kerr measurements, is the magnetization induced by iron in palladium, over a wide temperature range $5 \text{ K} < T < 300 \text{ K}$. The dimensional crossover we observe cannot be rationalized on the basis of structural considerations alone, since we find the dimensionality of the low temperature and of the critical region can differ. We discuss the crossover in terms of the temperature dependence of the magnon modes, giving rise to lower dimensionality at low temperatures.

(Some figures in this article are in colour only in the electronic version)

1. Introduction

The progress within the field of ultrathin magnets [1, 2] provides a unique testing ground for examining concepts of dimensionality and extension in condensed matter. One particularly fruitful approach has been to make contact with the statistical mechanical theory of critical phenomena [3] and search for experimental realizations of spin models. In the vicinity of the Curie point of a ferromagnetic transition, the thermodynamic observables associated with these models display universal characteristics, which may be parametrized in terms of critical exponents. These quantify how observables tend to zero or infinity at the transition and depend only on the range of the interactions, the symmetries of the Hamiltonian and the spatial dimensionality of the system.

Although the database of ultrathin experimental realizations of spin models is large and compelling [2, 4–6], reconciling the presence, in most cases, of itinerant electrons and complicated long-range interactions (such as the RKKY and dipolar couplings) with predictions based on localized nearest-neighbour spin models, remains problematic. Nevertheless, even when a direct comparison with a model Hamiltonian is lacking, it is beyond doubt that the low-dimensional structure of ultrathin magnets strongly alters their properties, compared to their bulk equivalents. In this respect, monitoring the dimensional crossover of a system as its thickness is reduced often provides a significant degree of insight. For example, a clear change from three- to two-dimensional critical exponents

has been observed in films of Ni on W(110) [7] and of Co on Cu(111) [8] as their thickness is reduced.

Here we examine a more subtle example of dimensional crossover, in which the dimensionality is not dictated by structural considerations alone. The material combination used for the exploration is δ -doped Pd(Fe), in which the dopant Fe is constrained to a single monolayer (ML) placed between two thicker (20 ML) Pd layers. Being easily polarizable, palladium develops a large magnetic moment by the presence of a magnetic impurity, such as iron. A single Fe impurity polarizes a region of Pd with a radius of roughly 10 \AA , giving rise to a magnetic moment corresponding to $10\text{--}12 \mu_B$ per Fe atom [9–11]. Calculations suggest the polarized region to be even larger in δ -doped Pd(Fe), extending up to 20 \AA from the Fe layers, corresponding to about 10 atomic planes of Pd(001) [12]. This is large compared to atomic scale imperfections such as steps, vacancies and defects. δ -doped Pd(Fe) systems therefore possess the appealing property of being magnetically ‘perfect’, even though structurally they may not be.

The influence of δ -doping on ferromagnetic ordering of Pd(Fe) was first studied experimentally by Pärnaste *et al* [13], who investigated the effect of the concentration of the Fe δ -doping on the ordering temperature and the dimensionality of the ferromagnetic transition. The behaviour of δ -doped layers differs markedly from conventional $\text{Fe}_x\text{Pd}_{1-x}$ alloys. As might be expected, both kinds display a pronounced increase in the ordering temperature with increasing Fe concentration.

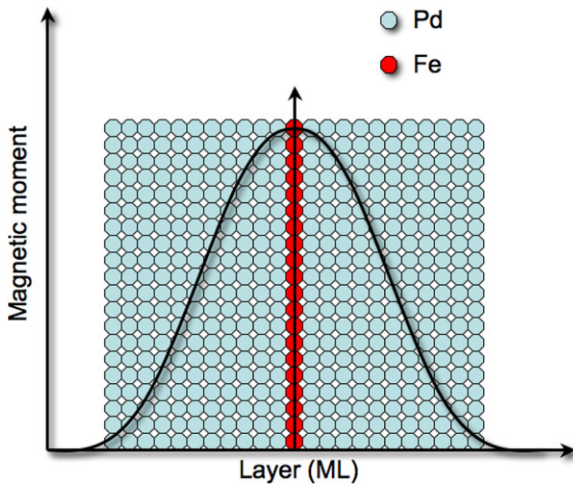


Figure 1. Schematic diagram of the decay in the magnetic moment from the central Fe (in red) layer in the surrounding Pd layers for an ideal stacked structure. The polarization of Pd extends for up to 10 monolayers.

However, the rate of change in the Curie temperature for equivalent changes in concentration for δ -doped alloys is over twice that of normal alloys [14]. In addition, Pärnaste *et al* reported a clear crossover from two- to three-dimensional critical behaviour in the measured remanent magnetization data for Fe thicknesses $d_{\text{Fe}} < 0.4$ ML.

The observation of this dimensionality crossover is, at first sight, surprising, since it is difficult to envisage three-dimensional behaviour arising from a ferromagnetic layer less than 1 ML thick. The key to understanding this phenomenon lies in the large polarizability sphere induced by the iron in the palladium. The width of the profile of the magnetic moment surrounding the central Fe layer is, at least to a first approximation, insensitive to the amount of Fe present, as illustrated in figure 1. This implies a fixed reference frame for magnon excitations in the direction perpendicular to the Fe monolayer (the z direction) between different samples. Therefore, provided the Curie temperature is sufficiently high, systems with d_{Fe} beyond a certain threshold can access these modes thermally, thus giving rise to three-dimensional critical behaviour.

The motivation of the present work is to experimentally verify whether this picture of magnons ‘freezing out’ can provide a consistent explanation for the behaviour of the magnetization over the full temperature range $5 \text{ K} < T < 300 \text{ K}$, and not only the critical region. An implication of this model is that the dimensionality of the critical region does not necessarily follow from that of the low temperature region. In principle, it should be possible to fabricate samples with δ -doping concentrations corresponding to three-dimensional critical behaviour and two-dimensional low temperature behaviour. Therefore, we have grown a set of samples with δ dopings corresponding to 0.5 and $1.4d_{\text{Fe}}$, and compare their behaviour with a three-dimensional reference sample in the form of a thick FePd alloy layer.

2. Experimental details

The δ -doped Pd(Fe) samples were grown using a DC magnetron sputtering method on a (100) MgO substrate. Samples were grown using a 10 ML vanadium seeding layer in order to alleviate a large lattice mismatch between Pd and MgO, and wetting. The Pd and Fe layers were deposited from sputtering targets of 99.99% purity for the relevant metal. The base pressure of the deposition system was 2×10^{-9} Torr, whereas the sputtering was carried out at a pressure of 2 mTorr.

The fcc Fe₁₀Pd₉₀ alloy sample was sputtered directly onto an Sr₂TiO₃ substrate. A 200 Å seeding layer of the alloy was first grown directly onto the substrate at a temperature of 700 °C. In this way, the alloy preferentially grows in large crystalline islands with (001) orientation. The sample was then cooled down to room temperature and a further 200 Å of the alloy deposited on top. This overlayer is polycrystalline, consisting of very small crystallites. These fill the vacancies on the surface of the seeding layer and ensure a smooth sample/vacuum interface. Subsequently, we annealed the sample at 600 °C for 30 min. During the annealing process, the crystallites in the topmost layer orient themselves along the direction of the seeding layer, whilst maintaining the smoothness of the surface/vacuum interface. The result of this process is a single-crystal (100) structure of an FePd alloy with very low surface roughness.

We investigated the magnetic properties of the films by means of the magneto-optic Kerr effect (MOKE) technique. The MOKE measurements were performed within a temperature range $5 \text{ K} < T < 300 \text{ K}$, using a longitudinal geometry set-up. A polarized laser light ($\lambda = 635 \text{ nm}$, $P = 30 \text{ mW}$) is used as a light source. The incident angle is fixed, $\theta = 41^\circ$. Strain-free ultra-high vacuum windows with negligible birefringence are positioned 30 cm from the maximum field. A Glan–Thompson prism is used to set the polarization of the incident beam to s-polarized light. The beam is reflected from the sample mounted on an He cryostat. The cryostat is equipped with a temperature controller with which we were able to control the temperature to within $\pm 0.02 \text{ K}$. The cryostat fits in the air gap of a quadrupole electromagnet capable of generating magnetic fields at the sample position of magnitude $\sim 600 \text{ mT}$. This configuration allows us to set the external magnetic field to any direction parallel to the sample surface without needing to change the scattering geometry.

The light reflected by the sample beam is modulated by a photoelastic modulator (PEM) operating at 50 kHz. The PEM retardation axis is placed parallel to the plane of incidence. The PEM allows simultaneous measurement of the first (Kerr ellipticity) and second (Kerr rotation) harmonic of the detected intensity of light and enables the study of the magnetic behaviour. The details of this technique have been described previously [15]. Two lock-in amplifiers were used to detect the first (50 kHz) and the second harmonic (100 kHz) of the reflected signal. The modulation retardation of the PEM is set at $\varphi = 175^\circ$ in order to maximize the amplitude of the second harmonic. The analyser is turned to $\pi/2$ parallel to the plane of incidence. Temperature-dependent hysteresis loops

were recorded by sweeping the current in the electromagnets with a slowly varying ($f = 0.4$ Hz) sine wave current and by means of a temperature controller. Before each measurement, a demagnetizing cycle for the quadrupole magnet was performed in order to avoid any remanent initial state of the magnetic field. The entire set-up is automatically controlled. The high modulation frequency (50 kHz), combined with the phase-sensitive amplification, allowed us an accurate and very sensitive registration of hysteresis loops, even on samples with extremely low Kerr rotation values, such as δ -doped Pd(Fe).

3. Results

We recorded ferromagnetic hysteresis loops over a series of temperatures $5 \text{ K} < T < 300 \text{ K}$ on samples of thickness $d_{\text{Fe}} = 0.5$ and 1.4 ML , and for the $\text{Fe}_{10}\text{Pd}_{90}$ alloy. Figure 2(a) displays a representative hysteresis loop for the 0.5 ML sample at 10 K . By recording similar loops over the entire temperature range, we can construct surface plots of the measured magnetization (Kerr rotation) as a function of temperature T and applied field H for the three samples (figures 2(b)–(d)). These allow us to make a number of qualitative observations. Firstly, there is a clear increase in the transition temperature T_c , below which spontaneous magnetic ordering occurs, with increasing Fe concentration. The rate of this increase as a function of Fe concentration is different for alloys and δ -doped samples, and our measured values are consistent with previous reports in the literature [13, 14]. Secondly, we notice a striking difference between the δ -doped and alloy samples along the $H = 0$ axis. In the δ -doped case there is a clear valley in the magnetization data all the way up to T_c . In the case of the alloy, however, this reduction in magnetization is considerably less pronounced at higher temperatures. Thus, different degrees of collinearity in the magnetization are anticipated in the samples.

At low temperature, we notice that for all three samples the ratio between the magnetization at saturation and at zero field is roughly 0.8. This is close to the theoretically predicted remanence value (0.834) [16] for polycrystalline fcc iron when the magnetization induced by an applied magnetic field lies in a random angle relative to the nearest cubic axis of the crystal. However, we can rule this possibility out, since we observed no change in hysteresis upon a 45° rotation of the field. In contrast, the ratio is known to be 0.5 when there is no preferred direction of magnetization in the sample [16]. Coupled with the fact that the valley at $H = 0$ disappears at higher temperatures for the alloy sample, we interpret this as indicative of a non-collinear contribution, possibly linked to dipolar interactions.

Above the ordering temperature, the field dependence is significantly different for these different classes of materials. The magnetic susceptibility ($\chi = \frac{\partial m}{\partial H}$) changes as $\chi_{\text{alloy}} \ll \chi_{1.4} \ll \chi_{0.5}$. This is an indication of the robustness of the transition to an external applied field and reflects the range of magnetic excitations in these samples.

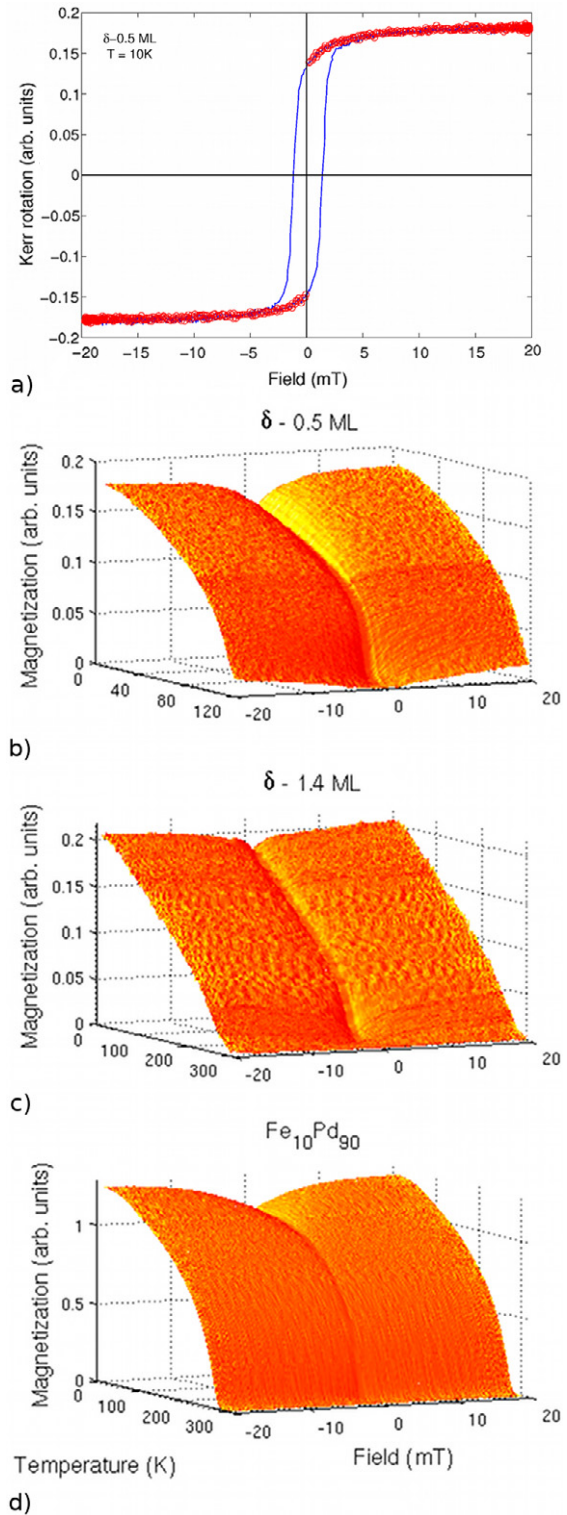


Figure 2. (a) Representative hysteresis loop recorded for the 0.5 ML sample at 10 K (solid blue line). The parts of the loop indicated by red circles have been used to create the surface plots below. Magnetization as a function of temperature and applied field for the (b) 0.5 and (c) 1.4 ML , and the (d) $\text{Fe}_{10}\text{Pd}_{90}$ alloy samples.

Critical temperature region

Although the qualitative differences in behaviour displayed in figure 2 are undoubtedly physical in origin, they highlight

a fundamental issue concerning the accessibility of the spontaneous magnetization M (also known as the order parameter) in experiments, and the relationship this has with measurable quantities such as the remanent magnetization, M_r , and the saturation magnetization, M_s .

At a continuous phase transition from ferro- to paramagnetism, the spontaneous magnetization, defined as the magnetization that exists within individual regions or domains of a system in zero applied field, vanishes according to a power law

$$M(T) = M_0 t^\beta, \quad (1)$$

where $t = (T_c - T)/T_c$ is the reduced temperature and β is the magnetization critical exponent. In practice, this quantity is hard to access experimentally using bulk probes, since these yield an average quantity which depends on the orientation of the magnetic domains. This difficulty makes a precise estimation of T_c problematic.

In this work, we follow the remanent magnetization, M_r , in order to get a handle on the behaviour of the spontaneous magnetization, and consequently we define T_c as the temperature at which M_r vanishes. Generally speaking this correspondence between M_r and M holds except at low temperatures, where there may be a number of geometrical and structural factors that contribute to a suppression of M_r with respect to the order parameter [17]. We emphasize that, as a result of these considerations, our reported values of the critical exponent β should be considered as effective. Nevertheless, we consider the obtained values as being useful in their own right, since they allow for a quantitative comparison between real samples as well as with model calculations. Figure 3 displays a log–log plot of M_r against t for the datasets extracted from figure 2, along with the determined β and T_c . The values of β we report were measured by choosing a T_c such that the range of the linear region in the log–log plot is maximized, an approach widely used by other authors [18–20, 7].

There are pronounced differences in behaviour between the three samples. Remarkably, the 0.5 ML sample displays power law behaviour over 2.5 decades in t , a strong indication of low dimensionality [3]. The 1.4 ML sample is characterized by a kink in the slope of the data at $\sim 0.5t$, and below that point the system appears to enter a separate low temperature regime that is also characterized by a linear behaviour in a log–log scale. We notice a similar, although much less pronounced, kink in the 0.5 ML data, at around $0.25t$. Finally, the $\text{Fe}_{10}\text{Pd}_{90}$ alloy data exhibits a behaviour consistent with a three-dimensional system, characterized by a conventional departure from critical behaviour at low temperatures.

We determined β to be 0.25(1), 0.44(1) and 0.55(1) for the 0.5, 1.4 ML and alloy samples, respectively. The $\beta = 0.25$ exponent measured in the 0.5 Fe ML system is slightly larger than the value characteristic of the 2dXY model on a finite lattice [21] ($\beta \simeq 0.23$) and is consistent with the values reported in [13]. We interpret this as further evidence for the two-dimensional nature of the $d_{\text{Fe}} = 0.5$ system in the vicinity of the critical temperature. The exponent obtained for the 1.4 ML sample, $\beta = 0.44(1)$, is considerably higher than values typical of 3d model systems, e.g. about 0.37 for the 3d Heisenberg model [22], and is larger than the previously

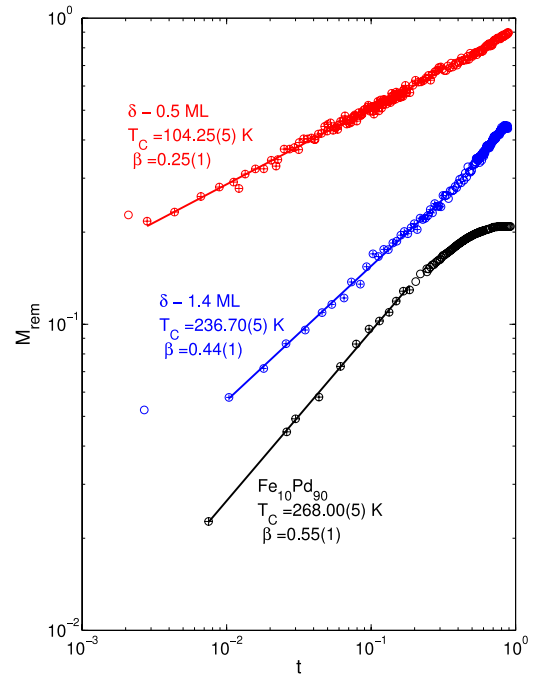


Figure 3. Log–log plot of the magnetic remanence of the $d_{\text{Fe}} = 0.5$, 1.4 ML and of $\text{Fe}_{10}\text{Pd}_{90}$ alloy as a function of the reduced temperature. The slope of the straight line gives the value of the effective critical exponent. The value β of 0.25 for the 0.5 Fe ML is comparable to that of the 2dXY model on a finite lattice [21].

reported value of 0.33 [13]. Nevertheless, this observation allows us to rule out two-dimensional critical behaviour for the 1.4 ML sample. Similarly, the alloy sample has a large effective β value, also consistent with bulk behaviour. We also note that previous measurements on Pd/Pd(1.2 at.% Fe)/Pd multilayers are consistent with two-dimensional Heisenberg behaviour down to 6.5 K [23]. While we cannot make a direct comparison with our data, this lends credence to our interpretation of our 3d samples in terms of the Heisenberg model.

Low temperature region

In order to explore the low temperature behaviour of the samples, we address the spontaneous and the saturation magnetization. In our analysis, we define this as $M_s = (M_+ - M_-)/2$, where M_+ and M_- are the averaged magnetizations within a field span from 12 to 20 mT of the positive and negative saturation fields, respectively. Our starting point is the expression

$$M_s(T) = M_s^0(1 - BT^c). \quad (2)$$

In three-dimensional ferromagnets, the thermal excitation of magnons leads to the celebrated Bloch $T^{3/2}$ law for the saturation magnetization [24]. It is straightforward to show that $c = 1$ for a two-dimensional system. Thus, in c one has a qualifier of the dimensionality of a system at low temperature. In addition, the constant B is known to be

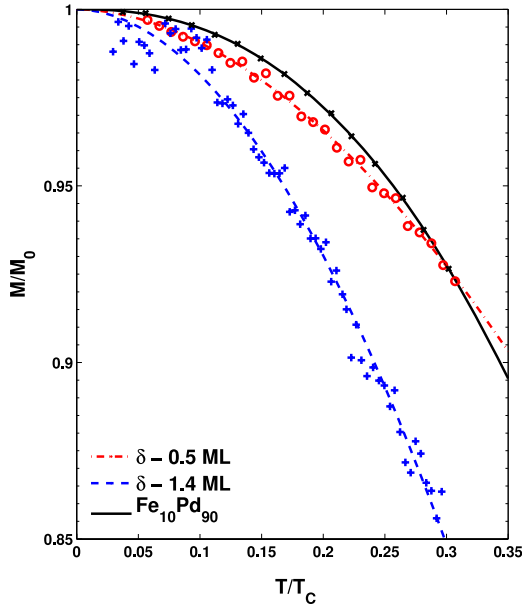


Figure 4. Temperature dependence of saturation magnetization $M_s(T)/M_s^0$ for 0.5 ML and 1.4 ML δ -doped FePd and the $\text{Fe}_{10}\text{Pd}_{90}$ alloy. The solid lines are fitting curves calculated from equation (2), with all three parameters varied in order to give the best fit.

Table 1. Estimated parameters for 0.5 ML and 1.4 ML δ -doped FePd, and for the $\text{Fe}_{10}\text{Pd}_{90}$ alloy, using equation (2) as a fitting function.

Sample	M_0	B	c
0.5 Fe ML	0.1821(1)	0.68(5)	1.86(4)
1.4 Fe ML	0.2039(1)	1.51(5)	1.91(4)
$\text{Fe}_{10}\text{Pd}_{90}$	1.2341(1)	1.27(5)	2.38(4)

inversely proportional to the spin wave stiffness, a measure of the energy cost necessary to thermally excite magnons [25].

We fitted the low temperature datasets (up to $0.3T_c$ in terms of the normalized temperature T/T_c) to equation (2) with B and c as fitting parameters. The results are summarized in table 1. A similar analysis was performed with data obtained from a linear extrapolation from high field to zero field in order to investigate high field susceptibility effects. The calculated values showed similar trends like the results of table 1 and thus do not change the following discussion.

The trend we observe for the exponent c is monotonic and increasing with Fe concentration, as shown in figure 4. Interestingly, however, the values are consistently larger than expected for a three-dimensional magnetic system. We suggest these should not be taken at face value, since it is likely that there are additional contributions that could make a $T^{3/2}$ law inappropriate in FePd systems. In particular, the Fe concentration provides an additional degree of freedom through which magnons may dissipate, as discussed below. Nevertheless, the considerably higher value of $c = 2.38(4)$ for the alloy sample indicates a different dimensionality compared to the δ -doped samples, whose values, $c = 1.86(4)$ and $1.91(4)$, are within experimental error of each other.

Turning to the constant B , we observe an increase in its value with Fe content in the case of δ -doped samples. In

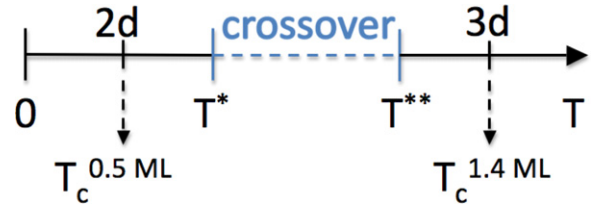


Figure 5. Schematic diagram depicting the placement of the critical temperatures of the studied samples with respect to the threshold temperatures T^* and T^{**} , which define the dimensionality crossover region for the critical behaviour of δ -doped Pd(Fe) layers.

particular, we find the coefficient for the 1.4 ML sample to be roughly 2.2 times larger than the one for the 0.5 ML sample. This suggests a relative softening of the magnon modes with increasing Fe concentration. For the alloy, on the other hand, the temperature dependence of the saturation magnetization is less pronounced and B decreases relative to the 1.4 ML value. This is to be expected, since the mean distance between Fe atoms increases again in the bulk sample with 10% Fe concentration.

4. Discussion

Let us start the discussion by recalling the quantized magnon model introduced in [13]. The hypothesis upon which the model rests, corroborated by first-principles calculations, is the fact that the width of the polarization profile surrounding the Fe layer is independent of the amount of Fe present. Consequently, the distance between the energy levels for the magnons in the direction perpendicular to the Fe layer remains fixed, regardless of Fe content. One can therefore imagine a fixed reference frame for the z magnon modes between samples with different δ dopings. Since the Fe concentration in the δ layer dictates the critical temperature T_c , increasing the level of doping makes the z magnon modes thermally accessible. Thus, the dimensionality of the ferromagnetic transition depends entirely on whether the critical temperature is above or below the crossover temperature at which the z magnon modes are excited.

In practice, the variation in the critical exponent β as a function of δ -doping measured experimentally [13] suggests a slightly more complex situation, shown schematically in figure 5. The threshold temperatures T^* and T^{**} delimit an extended crossover region, below which two-dimensional critical behaviour occurs and above which three-dimensional critical behaviour is manifest. The correspondence between Fe δ -doping and T_c allows us to identify the values of the threshold temperatures. The deviation from a 2d transition takes place at an Fe thickness of around 0.5 ML, corresponding to $T^* \sim 100$ K. Conversely, 3d behaviour is recovered when the Fe thickness is above 1 ML, corresponding to $T^{**} \sim 175$ K. This identifies the crossover region between 100 and 175 K, where the dimensionality is not well defined.

An important consequence of our model is that, provided the δ -doping concentration is high enough, the dimensionality crossover can occur within the same sample. If the Fe

concentration corresponds to a $T_c > T^{**}$, three-dimensional critical behaviour is observed. However, as the temperature decreases below T^* , one expects to measure two-dimensional behaviour. The 1.4 ML Fe sample, having an ordering temperature $T_c = 236.70(5)$ K that is above T^{**} , can be expected to be such a sample.

Our measurements over the full temperature range $5 \text{ K} < T < 300 \text{ K}$ allow us to test this hypothesis. By comparing the behaviour of the three samples, both in the low and critical temperature regimes, we may draw conclusions concerning their dimensionality.

In the 0.5 ML sample, we have persuasive evidence for two-dimensional behaviour both at low temperature and in the critical region. In the vicinity of T_c , the evidence is compelling and comes in the form of a large region over which power law behaviour is observed in reduced temperature, and the low value we extract for the critical exponent, $\beta = 0.25(1)$. At low temperature, we measure a small value for B , a constant reflecting the stiffness of magnons. Again, this is consistent with two-dimensional behaviour, since a slow suppression of the magnetization suggests stiffer magnon modes. Our estimate for the exponent $c = 1.86(4)$, is considerably higher than the theoretical prediction for a 2d system ($c = 1$). However, given the extra modes of dissipation present in Pd(Fe), and the fact that we measure an even higher value in the alloy sample, $c = 2.38(4)$, we also interpret this as indicative of a lower dimensionality.

Conversely, the $\text{Fe}_{10}\text{Pd}_{90}$ alloy sample behaves in a three-dimensional manner over the entire temperature range. In the critical region, the effective exponent $\beta = 0.55$ is not consistent with any of the dimensionality classes of model magnetism, but it allows us to confidently exclude a two-dimensional transition. In the low temperature region, we measure a large value of $c = 2.38(4)$, which, as remarked above, we also associate with three-dimensional behaviour.

We therefore take the 0.5 ML δ -doped and the $\text{Fe}_{10}\text{Pd}_{90}$ alloy samples as representative of the two-dimensional and three-dimensional limiting cases, respectively. We are now in a position to compare these to the behaviour of the 1.4 ML δ -doped sample. In the low temperature regime, we observe very little deviation from the 0.5 ML sample. In particular, the comparable c values reported in table 2 suggest the 1.4 ML system retains much of its low-dimensional character at low temperature. In the critical regime, however, we observe a strong departure from two-dimensional behaviour. We determine $\beta = 0.44(1)$, which is almost twice the value of the 0.5 ML sample, and comparable to the value measured for the alloy sample. Thus, we conclude the 1.4 ML δ -doped sample displays two-dimensional low temperature behaviour and three-dimensional critical behaviour. Our classification scheme for the entire sample set is summarized in table 2.

5. Conclusions

We have investigated a highly unusual instance of magnetic dimensional crossover, which does not rely solely on structural factors. The behaviour of Pd(Fe) δ -doped structures can only be rationalized by separating the atomic and magnetic

Table 2. Dimensionality classification for FePd samples.

Sample	Low T regime	Critical regime
0.5 Fe ML	2d	2d
1.4 Fe ML	2d	3d
Bulk $\text{Fe}_{10}\text{Pd}_{90}$	3d	3d

length scales. This is made possible because of the strong polarizability Fe induces in Pd. Thus, the giant moment ferromagnetism associated with FePd systems continues to surprise over 40 years since its discovery [9], by challenging the traditional notions of dimensional crossover in magnetism.

The crossover mechanism we propose for δ -doped Pd(Fe) systems is based on a quantized magnon model. We argue that two-dimensional behaviour only exists below a lower threshold temperature T^* , whereas three-dimensional behaviour occurs above a higher threshold temperature T^{**} . Thus, systems with a critical temperature below T^* , such as the 0.5 ML sample, display two-dimensional behaviour both in the low and critical temperature regime. On the other hand, systems with a critical temperature above T^{**} , such as the 1.4 ML sample, will display three-dimensional critical behaviour in the critical regime, but cross over to two-dimensional behaviour at low temperatures, below T^* . Our results therefore yield a consistent picture that allows us to classify the dimensionality of the Pd(Fe) δ -doped system, along with a conventional $\text{Fe}_{10}\text{Pd}_{90}$ alloy. This classification scheme is summarized in table 2.

The strong polarizability of palladium makes a direct comparison with model magnetism problematic. In this sense, the addition of iron can be viewed as an additional degree of freedom, to be considered alongside the system dimensionality. This may explain the systematically large c values we extract in equation (2). On the other hand, at low Fe concentrations we find compelling evidence for a recovery of model magnet behaviour, and find evidence suggesting the 0.5 ML sample behaves as a 2dXY ferromagnet on a finite lattice [21].

Finally, we remark that a direct measure of the magnon spectrum would be highly desirable in order to better understand the confinement effects we report in δ -doped Pd(Fe) systems. Although this is likely to be extremely challenging in practice, recent developments in spectroscopic techniques [26] do not rule this possibility out.

Acknowledgments

Financial support from the Icelandic Science Foundation and from the Swedish Foundation for International Cooperation in Research and Higher Education (STINT) is gratefully acknowledged. The authors acknowledge also the Knut and Alice Wallenberg Foundation for financing the development of the instruments used in this work.

References

- [1] Bland J A C and Heinrich B (ed) 2005 *Ultrathin Magnetic Structures* (Berlin: Springer)

- [2] Vaz C A F, Bland J A C and Lauhoff G 2008 Magnetism in ultrathin film structures *Rep. Prog. Phys.* **71** 0506501
- [3] Goldenfeld N 1992 *Lectures on Phase Transitions and the Renormalization Group (Frontiers in Physics Lecture Note Series)* (Colorado: Westview Press)
- [4] Elmers H J 1995 Ferromagnetic monolayers *Int. J. Mod. Phys. B* **9** 3115
- [5] Taroni A, Bramwell S T and Holdsworth P C W 2008 Universal window for two-dimensional critical exponents *J. Phys.: Condens. Matter* **20** 275233
- [6] Henkel M 1999 *Conformal Invariance and Critical Phenomena* (Berlin: Springer)
- [7] Li Y and Baberschke K 1992 Dimensional crossover in ultrathin Ni(111) films on W(110) *Phys. Rev. Lett.* **68** 1208
- [8] Huang F, Kief M T, Mankey G J and Willis R F 1994 Magnetism in the few monolayer limit: a surface magneto-optic Kerr-effect study of the magnetic behavior of ultrathin films of Co, Ni, and Co-Ni alloys on Cu(100) and Cu(111) *Phys. Rev. B* **49** 3962
- [9] Low G G and Holden T M 1966 Distribution of the ferromagnetic polarization induced by iron and cobalt ions in palladium *Proc. Phys. Soc.* **89** 119
- [10] Craig P P, Nagle D E, Steyert W A and Taylor R D 1962 Paramagnetism of Fe impurities in transition metals *Phys. Rev. Lett.* **9** 12
- [11] Nieuwenhuys G J 1975 Magnetic behaviour of cobalt, iron and manganese dissolved in palladium *Adv. Phys.* **24** 515
- [12] Holmström E, Nordström L and Niklasson A M N 2003 Giant magnetic enhancement in Fe/Pd films and its influence on the magnetic interlayer coupling *Phys. Rev. B* **67** 184403
- [13] Pärnaste M, Marcellini M, Holmström E, Bock N, Fransson J, Eriksson O and Hjörvarsson B 2007 Dimensionality crossover in the induced magnetization of Pd layers *J. Phys.: Condens. Matter* **19** 246213
- [14] Büscher C, Auerswald T, Scheer E, Schröder A, Löhneysen H v and Claus H 1992 Ferromagnetic transition in dilute Pd-Fe alloys *Phys. Rev. B* **46** 983-9
- [15] Sato K 1981 Measurement of magneto-optical Kerr effect using piezo-birefringent modulator *Japan. J. Appl. Phys.* **20** 2403
- [16] Bozorth R M (ed) 1993 *Ferromagnetism* (New York: IEEE Press)
- [17] Pouloupoulos P and Baberschke K 1999 Magnetism in thin films *J. Phys.: Condens. Matter* **11** 9495
- [18] Dürr W, Taborelli M, Paul O, Germar R, Gudat W, Pescia D and Landolt M 1989 Magnetic phase transition in two-dimensional ultrathin Fe films on Au(100) *Phys. Rev. Lett.* **62** 206
- [19] Liu C and Bader S D 1990 Two-dimensional magnetic phase transition of ultrathin iron films on Pd(100) *J. Appl. Phys.* **67** 5758
- [20] Connelly D L, Loomis J S and Mapother D E 1971 Specific heat of nickel near the Curie temperature *Phys. Rev. B* **3** 924-34
- [21] Bramwell S T and Holdsworth P C W 1993 Magnetization and universal sub-critical behaviour in two-dimensional *xy* magnets *J. Phys.: Condens. Matter* **5** L53-9
- [22] Campostrini M, Hasenbusch M, Pelissetto A, Rossi P and Vicari E 2002 Critical exponents and equation of state of the three-dimensional Heisenberg universality class *Phys. Rev. B* **65** 144520
- [23] Webb D J and McKinley J D 1993 Two-dimensional magnetism in Pd (1.2 at.% Fe) films *Phys. Rev. Lett.* **70** 509-12
- [24] Bloch F 1930 Zur theorie des ferromagnetismus *Z. Phys.* **61** 206
- [25] Stöhr J and Siegmann H C 2006 *Magnetism: From Fundamentals to Nanoscale Dynamics* (Berlin: Springer)
- [26] Prokop J, Tang W X, Zhang Y, Tudosa I, Peixoto T R F, Zakeri Kh and Kirschner J 2009 Magnons in a ferromagnetic monolayer *Phys. Rev. Lett.* **102** 177206